Analytical and Numerical Solutions of the Relativistic Schrödinger Differential Wave Equation

James H. McNeill, Natural Sciences Department, Middle Georgia State University, Macon, GA 31206, USA

James E. Bidlack*, Department of Biology, University of Central Oklahoma, Edmond, OK 73034, USA

Abstract: This paper discusses the relativistic Schrödinger differential wave equation for the hydrogen atom and hydrogen-like cations, which have measured ionization energies from hydrogen to the Cu^{28+} hydrogen-like cation. The analytical solution to the relativistic Schrödinger differential wave equation correlates with experimental data if the angular momentum quantum number $l > 0$. For quantum levels with $l = 0$, the analytical solutions predict ionization energy values larger than that measured for the hydrogen atom and hydrogen-like cations. Also, beyond the element erbium, $Z > 68$ for $l=0$ quantum states, the analytical solution yields energy values that are complex numbers. This is similar for the Dirac relativistic differential wave equation which fails for nuclei that have an atomic number larger than 137. Using measured 1*s* ionization energy values of hydrogen-like cations, a numerical solution to the relativistic Schrödinger differential wave equation is possible since an analytical one is not when the measured ionization energy is different from the analytical result. In addition, since the analytical solutions to the radial part of the relativistic Schrödinger differential wave equation are complicated, normalized numerical solutions are less difficult to obtain using Microsoft Excel. Most differential equations do not have analytical solutions, and, therefore, only numerical solutions are possible utilizing boundary or initial conditions.

Classical Schrödinger Differential Wave Equation and Wave-Particle Duality in Quantum Mechanics

The authors are a nuclear chemist and a plant physiologist, interested in the chemical physics of our natural world, with previous publications in this journal about similar topics (McNeill and Bidlack, 2018; McNeill et al., 2021). This paper focuses on the subtle effects of the *Special Theory of Relativity* (Einstein, 1905a; 1905b; 1905c; 1905d) upon atomic structure. As such, the larger the atomic number, Z, the greater the relativistic effect may be on how atoms exist.

The classical Hamiltonian for any particle in motion bound by a negative potential $-U$, such as the negative gravitational potential between a planet orbiting the sun, has a constant mechanical energy value E_m less than zero (Kleppner and Kolenkow, 2014). In classical Newtonian physics for a planet orbiting the sun, the total mechanical energy E_m is the kinetic energy $KE = \frac{1}{2}m_p v^2$, where m_p is the rest mass of the moving planet in kilograms and v is the speed or magnitude in units of meters per second of the planet's velocity vector $\mathbf{v}$ orbiting the sun, plus the energy value of the negative gravitational potential energy $-U$.

*Corresponding author: jbidlack@uco.edu

$$KE + (-U) = \frac{1}{2}m_p v^2 + \left(-\frac{GM_S m_p}{r}\right) = \frac{m_p^2 v^2}{2m_p} - \frac{GM_S m_p}{r} = \frac{p_p^2}{2m_p} - \frac{GM_S m_p}{r} = E_m < 0 \quad (1)$$

In Equation 1, the p_p^2 is the squared magnitude of the planet's momentum vector $\mathbf{p}_p = m_p\mathbf{v}$, M_s is the rest mass of the sun in kilograms, r is the separation distance in meters from the center-of-mass of the planet to that of the sun, and G is the gravitational constant which can only be measured to four significant figures.

$$G = 6.673 \times 10^{-11} \frac{\text{m}^3}{\text{kg s}^2} \text{ (Kleppner and Kolenkow, 2014)} \quad (2)$$

If the value of the mechanical energy E_m is equal to or greater than zero ($E_m \geq 0$), the planet is unbound and can escape from the negative potential of the sun's gravitational force due to sufficient kinetic energy of motion.

For the electron in the hydrogen atom, or hydrogen-like cations that have only one electron and more than one proton in the atomic nucleus, the negative gravitational potential is replaced in Equation 1 by the negative Coulomb potential between the negatively charged electron and the positively charged atomic nucleus.

$$\frac{p^2}{2m_e} - \frac{1}{4\pi\varepsilon_0}\frac{Zq^2}{r} = E_m \text{ where the negative potential } -U \text{ is } -U = -\frac{1}{4\pi\varepsilon_0}\frac{Zq^2}{r} \quad (3)$$

In the above equation, m_e is the measured mass of an electron at rest in kilograms

$$m_e = 9.10938 \times 10^{-31} \text{ kilogram (Tipler and Llewellyn, 2012)} \quad (4)$$

And ε_0 is the electrostatic permittivity of a vacuum which in MKS units is measured to be the numerical value shown below.

$$\varepsilon_0 = 8.854187817 \times 10^{-12} \frac{\text{Coulomb}^2\,\text{second}^2}{\text{kilogram meter}^3} \text{ (Tipler and Llewellyn, 2012)} \quad (5)$$

Z is the atomic number or number of protons in the atomic nucleus, and q is the measured magnitude of charge for both the electron and proton expressed in units of the Coulomb.

$$q = 1.602177 \times 10^{-19} \text{ Coulomb (Tipler and Llewellyn, 2012)} \quad (6)$$

In addition, r is the distance between the centers-of-mass of the electron and atomic nucleus in meters, analogous to the orbiting planet and sun in the gravitational potential.

In quantum mechanics, subatomic particles have wave-particle duality as photons of light (Tipler and Llewellyn, 2012). The wavelength λ, is directly proportional to the reciprocal of the magnitude $p = mv$ of the momentum vector $\mathbf{p} = m\mathbf{v}$ for any subatomic particle or a photon of light with Planck's constant h as the measured proportionality constant (numerical value from Tipler and

Llewellyn, 2012).

$$\lambda = \frac{h}{p} = \frac{h}{mv} \text{ and } h = 6.62607 \times 10^{-34} \text{ Joule seconds or } \frac{\text{kg m}^2}{\text{sec}} \text{ in meters, kilograms and seconds (MKS)units} \quad (7)$$

For the above equation, mass is in kilograms, speed in meters per second, and wavelength in meters. The time-independent wave function ψ for a freely moving subatomic particle or a photon of light is the real part of the next equation.

$$\psi = \psi(r) = e^{ikr} \text{ where } k = \frac{2\pi}{\lambda} = \frac{2\pi}{h}mv = \frac{p}{\hbar} \text{ and } \hbar = \frac{h}{2\pi} = 1.05457 \times 10^{-34} \frac{\text{kg m}^2}{\text{sec}} \text{ (Walker et al., 2014)} \quad (8)$$

Therefore, the second derivative of the wave function yields the following equation for the vector dot product of the momentum vector $\mathbf{p} \bullet \mathbf{p} = p^2$ of such a moving particle displaying wave-particle duality.

$$\frac{d^2\psi}{dr^2} = -\frac{p^2}{\hbar^2}\psi \quad \text{So } p^2\psi = -\hbar^2\frac{d^2\psi}{dr^2} \quad (9)$$

Thus, using the expression ψ for the wave function of an electron in a hydrogen atom or a hydrogen-like cation by the substitution of Equation 9 for the classical kinetic energy in Equation 3, one arrives at the classical Schrödinger differential wave equation for the single electron in a hydrogen atom or hydrogen-like cation.

$$-\frac{\hbar^2}{2m_e}\nabla^2\psi - \frac{1}{4\pi\varepsilon_0}\frac{Zq^2}{r}\psi = E_m\psi \quad (10)$$

In addition, the electron motion is a three-dimensional wave encircling the atomic nucleus, resulting in taking the double derivative of the wave function ψ with respect to each of the three rectangular coordinates *x, y,* and *z*. In Equation 10, ∇^2 is the following dot product of the vector operator $\boldsymbol{\nabla}$.

$$\nabla^2\psi = \boldsymbol{\nabla}\cdot\boldsymbol{\nabla}\psi = \left[\frac{\partial}{\partial x}\hat{\mathbf{x}} + \frac{\partial}{\partial y}\hat{\mathbf{y}} + \frac{\partial}{\partial z}\hat{\boldsymbol{z}}\right]\cdot\left[\frac{\partial}{\partial x}\hat{\mathbf{x}} + \frac{\partial}{\partial y}\hat{\mathbf{y}} + \frac{\partial}{\partial z}\hat{\boldsymbol{z}}\right]\psi = \frac{\partial^2\psi}{\partial x^2} + \frac{\partial^2\psi}{\partial y^2} + \frac{\partial^2\psi}{\partial z^2} \text{ (Walker et al., 2014)} \quad (11)$$

In the rectangular coordinate system with the center of the nucleus being at the origin, the magnitude for the distance between centers-of-mass of the electron and the atomic nucleus can be expressed as

$$r = (x^2 + y^2 + z^2)^{1/2} = \sqrt{x^2 + y^2 + z^2} \quad (12)$$

It is necessary to transform the ∇^2 operator into spherical-polar coordinates r, θ, and ϕ to obtain an analytical solution. First, there is the position vector **r**, with a magnitude equal to the separation distance from the center-of-mass of the atomic nucleus to the electron's center-of-mass, given in the next expression (Wangsness, 1986).

$$\mathbf{r} = r\hat{\mathbf{r}} = r[\cos\phi \sin\theta\, \hat{\mathbf{x}} + \sin\phi \sin\theta\, \hat{\mathbf{y}} + \cos\theta\, \hat{\mathbf{z}}] = r\cos\phi \sin\theta\, \hat{\mathbf{x}} + r\sin\phi \sin\theta\, \hat{\mathbf{y}} + r\cos\theta\, \hat{\mathbf{z}} \quad (13)$$

In Equation 13, $\hat{\mathbf{r}}$ is a unit vector like the orthonormal unit vectors $\hat{\mathbf{x}}$, $\hat{\mathbf{y}}$, and $\hat{\mathbf{z}}$ in rectangular coordinates. The angle between the z-axis and vector $\mathbf{r}$ is the spherical-polar coordinate θ. The angle between the projection of vector $\mathbf{r}$ ($r\sin\theta$) onto the xy-plane, at z=0, and the x-axis is ϕ.

Using the chain rule in differential calculus, $\nabla\psi$ is the following expression.

$$\nabla\psi = \left[\frac{\partial\psi}{\partial r}\frac{\partial r}{\partial x} + \frac{\partial\psi}{\partial\theta}\frac{\partial\theta}{\partial x} + \frac{\partial\psi}{\partial\phi}\frac{\partial\phi}{\partial x}\right]\hat{\mathbf{x}} + \left[\frac{\partial\psi}{\partial r}\frac{\partial r}{\partial y} + \frac{\partial\psi}{\partial\theta}\frac{\partial\theta}{\partial y} + \frac{\partial\psi}{\partial\phi}\frac{\partial\phi}{\partial y}\right]\hat{\mathbf{y}} + \left[\frac{\partial\psi}{\partial r}\frac{\partial r}{\partial z} + \frac{\partial\psi}{\partial\theta}\frac{\partial\theta}{\partial z} + \frac{\partial\psi}{\partial\phi}\frac{\partial\phi}{\partial z}\right]\hat{\mathbf{z}} \quad (14)$$

Table I displays the partial derivatives of each of the three spherical-polar coordinates with respect to each of the three rectangular coordinates. In addition to unit vector $\hat{\mathbf{r}}$, there are two additional unit vectors $\hat{\boldsymbol{\theta}}$ and $\hat{\boldsymbol{\phi}}$ in spherical-polar coordinates, and all three are likewise orthonormal as $\hat{\mathbf{x}}$, $\hat{\mathbf{y}}$, and $\hat{\mathbf{z}}$ in rectangular coordinates.

$$\hat{\boldsymbol{\theta}} = \frac{\partial\hat{\mathbf{r}}}{\partial\theta} = \cos\phi\cos\theta\, \hat{\mathbf{x}} + \sin\phi\cos\theta\, \hat{\mathbf{y}} - \sin\theta\, \hat{\mathbf{z}} \qquad \hat{\boldsymbol{\phi}} = \frac{1}{\sin\theta}\frac{\partial\hat{\mathbf{r}}}{\partial\phi} = -\sin\phi\, \hat{\mathbf{x}} + \cos\phi\, \hat{\mathbf{y}} \text{ (Wangsness, 1986)} \quad (15)$$

Table I Partial Derivatives of Spherical-Polar Coordinates with Respect to Rectangular Coordinates

$$\frac{\partial r}{\partial x} = \frac{\partial}{\partial x}\left[(x^2 + y^2 + z^2)^{1/2}\right] = \cos\phi \sin\theta$$

$$\frac{\partial r}{\partial y} = \frac{\partial}{\partial y}\left[(x^2 + y^2 + z^2)^{1/2}\right] = \sin\phi \sin\theta$$

$$\frac{\partial r}{\partial z} = \frac{\partial}{\partial z}\left[(x^2 + y^2 + z^2)^{1/2}\right] = \cos\theta$$

$$\frac{\partial\theta}{\partial x} = \frac{\partial}{\partial x}\text{arccosine}\left[\frac{z}{(x^2 + y^2 + z^2)^{1/2}}\right] = \frac{1}{r}\cos\phi\cos\theta$$

$$\frac{\partial\theta}{\partial y} = \frac{\partial}{\partial y}\text{arccosine}\left[\frac{z}{(x^2 + y^2 + z^2)^{1/2}}\right] = \frac{1}{r}\sin\phi\cos\theta$$

$$\frac{\partial\theta}{\partial z} = \frac{\partial}{\partial z}\text{arccosine}\left[\frac{z}{(x^2 + y^2 + z^2)^{1/2}}\right] = -\frac{1}{r}\sin\theta$$

$$\frac{\partial\phi}{\partial x} = \frac{\partial}{\partial x}\text{arccosine}\left[\frac{x}{(x^2 + y^2)^{1/2}}\right] = -\frac{1}{r}\frac{\sin\phi}{\sin\theta}$$

$$\frac{\partial\phi}{\partial y} = \frac{\partial}{\partial y}\text{arcsine}\left[\frac{y}{(x^2 + y^2)^{1/2}}\right] = \frac{1}{r}\frac{\cos\phi}{\sin\theta}$$

$$\frac{\partial\phi}{\partial z} = \frac{\partial}{\partial z}\text{arcsine}\left[\frac{y}{(x^2 + y^2)^{1/2}}\right] = 0$$

Using the chain rule with the partial derivatives displayed in Table I for Equation 14, $\boldsymbol{\nabla}\psi$ is the next expression in spherical-polar coordinates, transformed from rectangular coordinate unit vectors into spherical-polar coordinate unit vectors, after collection of terms that have rectangular coordinate unit vectors comprising the spherical-polar coordinate unit vectors.

$$\boldsymbol{\nabla}\psi = \left[\frac{\partial}{\partial x}\hat{\mathbf{x}} + \frac{\partial}{\partial y}\hat{\mathbf{y}} + \frac{\partial}{\partial z}\hat{\mathbf{z}}\right]\psi = \left[\hat{\mathbf{r}}\frac{\partial}{\partial r} + \hat{\boldsymbol{\theta}}\frac{1}{r}\frac{\partial}{\partial \theta} + \hat{\boldsymbol{\phi}}\frac{1}{r\sin\theta}\frac{\partial}{\partial \phi}\right]\psi \tag{16}$$

The following vector dot product can then be used to transform Equation 11 from rectangular coordinates to spherical-polar coordinates.

$$\nabla^2\psi = \boldsymbol{\nabla}\cdot\boldsymbol{\nabla}\psi = \left[\hat{\mathbf{r}}\frac{\partial}{\partial r} + \hat{\boldsymbol{\theta}}\frac{1}{r}\frac{\partial}{\partial \theta} + \hat{\boldsymbol{\phi}}\frac{1}{r\sin\theta}\frac{\partial}{\partial \phi}\right]\cdot\left[\hat{\mathbf{r}}\frac{\partial}{\partial r} + \hat{\boldsymbol{\theta}}\frac{1}{r}\frac{\partial}{\partial \theta} + \hat{\boldsymbol{\phi}}\frac{1}{r\sin\theta}\frac{\partial}{\partial \phi}\right]\psi \tag{17}$$

In Equation 17, it is important to note that unit vectors $\hat{\mathbf{r}}$ and $\hat{\boldsymbol{\theta}}$ are functions of θ and ϕ, as unit vector $\hat{\boldsymbol{\phi}}$ is a function of ϕ when performing the dot product of $\boldsymbol{\nabla}\cdot\boldsymbol{\nabla}\psi$ (see Table II). It is necessary to take the partial derivatives of these three spherical polar coordinate unit vectors while conducting this vector dot product. After performing the vector dot-product in Equation 17 and algebraic rearrangement, one has $\nabla^2\psi$ transformed into spherical polar coordinates.

$$\nabla^2\psi = \left[\frac{\partial^2}{\partial x^2} + \frac{\partial^2}{\partial y^2} + \frac{\partial^2}{\partial z^2}\right]\psi = \left[\frac{1}{r^2}\frac{\partial}{\partial r}\left(r^2\frac{\partial}{\partial r}\right) + \frac{1}{r^2\sin\theta}\frac{\partial}{\partial \theta}\left(\sin\theta\frac{\partial}{\partial \theta}\right) + \frac{1}{r^2\sin^2\theta}\frac{\partial^2}{\partial \phi^2}\right]\psi \tag{18}$$

Table II Partial Derivatives in Equation 17 not Equal to Zero

$$\frac{\partial\hat{\mathbf{r}}}{\partial\theta} = \cos\phi\cos\theta\,\hat{\mathbf{x}} + \sin\phi\cos\theta\,\hat{\mathbf{y}} - \sin\theta\,\hat{\mathbf{z}} = \hat{\boldsymbol{\theta}}$$

$$\frac{\partial\hat{\boldsymbol{\theta}}}{\partial\theta} = -\cos\phi\sin\theta\,\hat{\mathbf{x}} - \sin\phi\sin\theta\,\hat{\mathbf{y}} - \cos\theta\,\hat{\mathbf{z}} = -\hat{\mathbf{r}}$$

$$\frac{\partial\hat{\mathbf{r}}}{\partial\phi} = -\sin\phi\sin\theta\,\hat{\mathbf{x}} + \cos\phi\sin\theta\,\hat{\mathbf{y}} = (-\sin\phi\,\hat{\boldsymbol{x}} + \cos\phi\,\hat{\boldsymbol{y}})\sin\theta = \sin\theta\,\hat{\boldsymbol{\phi}}$$

$$\frac{\partial\hat{\boldsymbol{\theta}}}{\partial\phi} = -\sin\phi\cos\theta\,\hat{\mathbf{x}} + \cos\phi\cos\theta\,\hat{\mathbf{y}} = (-\sin\phi\,\hat{\mathbf{x}} + \cos\phi\,\hat{\mathbf{y}})\cos\theta = \cos\theta\,\hat{\boldsymbol{\phi}}$$

$$\frac{\partial\hat{\boldsymbol{\phi}}}{\partial\phi} = -\cos\phi\,\hat{\mathbf{x}} - \sin\phi\,\hat{\mathbf{y}}$$

The classical Schrödinger differential wave equation is appropriate when the electron in an atom never approaches the speed of light. However, for large nuclei, such as lead (Pb) with an atomic number of 82 or 82 protons, the electrons with the angular momentum quantum number l=0 approach the speed of light as they come into close contact with the nucleus. Theoretically, electrons that have angular momentum quantum number equal to zero, in classical physics, have linear oscillatory motion (Walker et al., 2014) and penetrate through the atomic nucleus twice during each oscillation. Thus, it is necessary to evaluate the relativistic Schrödinger differential wave equation for such large nuclei.

Einstein's Special Theory of Relativity and the Relativistic Schrödinger Differential Wave Equation

By Einstein's Special Theory of Relativity, kinetic energy, KE, is equal to the difference between the relativistic mass m_{re} of an electron multiplied by the speed-of-light squared c^2 and the electron rest mass m_e times the speed-of-light squared.

$$KE = m_{re}c^2 - m_e c^2 \text{ (Tipler and Llewellyn, 2012)} \tag{19}$$

Concisely, the speed of light in units of meters per second is the following large integer number.

$$c = 299{,}792{,}458 \frac{\text{meters}}{\text{second}} \text{ (Tipler and Llewellyn, 2012)} \tag{20}$$

And the relativistic mass m_{re} of the electron is equal to the electron rest mass m_e divided by the square-root of the quantity $1-v^2/c^2$, where v is the speed of the electron and c is the speed of light.

$$m_{re} = \frac{m_e}{\sqrt{1 - v^2/c^2}} = \frac{m_e}{(1 - v^2/c^2)^{1/2}} \text{ (Tipler and Llewellyn, 2012)} \tag{21}$$

Therefore, the Hamiltonian, kinetic energy plus negative potential energy, for the electron in a hydrogen atom or hydrogen-like cation becomes the following expression when using Equation 19 to express the kinetic energy of the electron.

$$(m_{re}c^2 - m_e c^2) - \frac{1}{4\pi\varepsilon_0}\frac{Zq^2}{r} = E_m \tag{22}$$

And Equation 22 can be rearranged into the following more convenient expression.

$$m_{re}c^2 - \frac{1}{4\pi\varepsilon_0}\frac{Zq^2}{r} = E_m + m_e c^2 = E_s \tag{23}$$

E_s is the energy sum or sum of the electron rest mass energy $m_e c^2$ and the mechanical energy E_m. $E_s$can only be a positive number and greater than zero (E_s>0) when including angular momentum. If the sum energy E_s=0, then E_m=$-m_e c^2$, and the relativistic energy of the orbiting electron becomes equal to the magnitude of the negative Coulomb potential.

$$m_{re}c^2 = \frac{1}{4\pi\varepsilon_0}\frac{Zq^2}{r} \tag{24}$$

In classical physics, if an electron in a hydrogen-like cation has a perfectly circular orbit, the centrifugal force for the relativistic electron in motion equals the magnitude of the Coulomb force of attraction.

$$m_{re}\frac{v^2}{r} = \frac{1}{4\pi\varepsilon_0}\frac{Zq^2}{r^2} \tag{25}$$

Next, multiply both sides of Equation 25 with distance r

$$m_{re}v^2 = \frac{1}{4\pi\varepsilon_0}\frac{Zq^2}{r} (= m_{re}c^2 \text{ because } v = c \text{ when } E_s = 0) \tag{26}$$

Hence, when E_s=0 and the centrifugal force equals the magnitude of the attractive Coulomb force, the relativistic electron moves at the speed-of-light with a relativistic mass equal to infinity, which would only be possible if the electron and atomic nucleus were both point masses and separation distance r=0. This is one explanation of why the sum energy E_s is greater than zero, and the mechanical energy E_m is greater than the negative electron rest mass energy ($E_m > -m_e c^2$). In addition, if one squares the result in Equation 24

$$\frac{m_e^2 c^4}{1 - v^2/c^2} = \left(\frac{1}{4\pi\varepsilon_0}\frac{Zq^2}{r}\right)^2 \tag{27}$$

Then Equation 27 can be rearranged into the next expression.

$$\left(\frac{1}{4\pi\varepsilon_0}\frac{Zq^2}{r}\right)^2 \frac{v^2}{c^2} = \left(\frac{1}{4\pi\varepsilon_0}\frac{Zq^2}{r}\right)^2 - m_e^2 c^4 \tag{28}$$

Afterwards, substitute the result of Equation 24 into Equation 28 to arrive at

$$m_{re}^2 v^2 c^2 = p_{re}^2 c^2 = m_{re}^2 c^4 - m_e^2 c^4 \tag{29}$$

Where in Equation 29, p_{re} is the magnitude of the relativistic momentum $\mathbf{p}_{re}$=$m_{re}\mathbf{v}$ of the electron in motion such that

$$\mathbf{p}_{re} = \frac{m_e}{\sqrt{1 - v^2/c^2}}\mathbf{v} \text{ (Tipler and Llewellyn, 2012)} \tag{30}$$

The expression in Equation 29 is derived from the following famous equation in Einstein's Special Theory of Relativity.

$$E = m_{re}c^2 = \frac{m_e c^2}{\sqrt{1 - v^2/c^2}} = \frac{m_e c^2}{(1 - v^2/c^2)^{1/2}} \text{ (Tipler and Llewellyn, 2012)} \tag{31}$$

For energy levels with angular momentum, this is another explanation why the sum energy E_s can only be a positive number greater than zero and the mechanical energy E_m must be larger than the negative electron rest mass energy.

If one adds the electron rest mass energy squared $m_e^2 c^4$ on both sides of Equation 29, and then takes the square-root of both sides, the next expression is the result.

$$m_{re}c^2 = \sqrt{p_{re}^2 c^2 + m_e^2 c^4} = (p_{re}^2 c^2 + m_e^2 c^4)^{1/2} \tag{32}$$

This result of Equation 32 is then substituted in Equation 23 for the electron's relativistic mass energy $m_{re}c^2$.

$$\sqrt{p_{re}^2 c^2 + m_e^2 c^4} - \frac{1}{4\pi\varepsilon_0}\frac{Zq^2}{r} = E_s \tag{33}$$

To use the squared momentum operator in Equation 33 above, the Coulomb potential is added to both sides of the equation, and then squaring both sides of the equation to obtain the next relation.

$$p_{re}^2 c^2 + m_e^2 c^4 = \left(E_s + \frac{1}{4\pi\varepsilon_0}\frac{Zq^2}{r}\right)^2 = E_s^2 + 2E_s\frac{1}{4\pi\varepsilon_0}\frac{Zq^2}{r} + \left(\frac{1}{4\pi\varepsilon_0}\frac{Zq^2}{r}\right)^2 \tag{34}$$

Then, subtract the square of the rest mass energy $m_e^2c^4$ of the electron from both sides of Equation 34 and square the Coulomb potential to arrive at the next expression.

$$p_{re}^2c^2 = (E_s^2 - m_e^2c^4) + 2E_s\frac{1}{4\pi\varepsilon_0}\frac{Zq^2}{r} + \frac{1}{(4\pi\varepsilon_0)^2}\frac{Z^2q^4}{r^2} \tag{35}$$

Now when using the dot product of the momentum operator ∇^2, the relativistic version of the Schrödinger differential wave equation becomes the next differential expression.

$$-\hbar^2c^2\nabla^2\psi = \left[(E_s^2 - m_e^2c^4) + 2E_s\frac{1}{4\pi\varepsilon_0}\frac{Zq^2}{r} + \frac{1}{(4\pi\varepsilon_0)^2}\frac{Z^2q^4}{r^2}\right]\psi \tag{36}$$

After dividing Equation 36 by squared product $\hbar^2c^2$ and rearranging this equation to equal zero

$$-\nabla^2\psi - \left[\frac{E_s^2 - m_e^2c^4}{\hbar^2c^2} + \frac{2E_s}{\hbar^2c^2}\frac{1}{4\pi\varepsilon_0}\frac{Zq^2}{r} + \frac{1}{\hbar^2c^2(4\pi\varepsilon_0)^2}\frac{Z^2q^4}{r^2}\right]\psi = 0 \tag{37}$$

The expression in Equation 37 can be further simplified by substitution of the following unitless term α such that

$$\alpha = \frac{q^2}{\hbar c 4\pi\varepsilon_0} = \frac{(1.602177\times10^{-19}\ \text{Coulomb})^2}{\left(1.05457\times10^{-34}\frac{\text{kg m}^2}{\text{sec}}\right)\left(299{,}792{,}458\frac{\text{m}}{\text{sec}}\right)4\pi\left(8.854187817\times10^{-12}\frac{\text{Coul}^2\text{sec}^2}{\text{kg m}^3}\right)} = \frac{1}{137.036} \tag{38}$$

to obtain the next expression.

$$-\nabla^2\psi - \left[\frac{E_s^2 - m_e^2c^4}{\hbar^2c^2} + \frac{2E_s}{\hbar c}\frac{Z\alpha}{r} + \frac{Z^2\alpha^2}{r^2}\right]\psi = 0 \tag{39}$$

The unitless numerical reciprocal of 137.036 in Equation 38 is calculated using the numerical values with units given in Equations 2, 8, 9 and 20. The relativistic version of the Schrödinger differential wave equation is now the following expression in terms of spherical-polar coordinates.

$$-\frac{1}{r^2}\frac{\partial}{\partial r}\left(r^2\frac{\partial\psi}{\partial r}\right) - \frac{1}{r^2\sin\theta}\frac{\partial}{\partial\theta}\left(\sin\theta\frac{\partial\psi}{\partial\theta}\right) - \frac{1}{r^2\sin^2\theta}\frac{\partial^2\psi}{\partial\phi^2} - \left[\frac{E_s^2 - m_e^2c^4}{\hbar^2c^2} + \frac{2E_s}{\hbar c}\frac{Z\alpha}{r} + \frac{Z^2\alpha^2}{r^2}\right]\psi = 0 \tag{40}$$

Equation 40 is a linear, nonhomogeneous partial differential equation that may have an analytical solution (Walker et al., 2014) by separation of variables r, θ, and ϕ when setting $\psi(r,\theta,\phi)=R(r)\Theta(\theta)\Phi(\phi)$, the product of three separate different functions of the spherical-polar coordinates. It is obvious that the analytical solution for the differential expression of θ and ϕ are the same as in the classical Schrödinger differential wave equation (Walker et al., 2014). The analytical solution for angle ϕ is the following simple exponential function.

$$\Phi(\phi) = e^{\pm im_l\phi} \tag{41}$$

In Equation 41, m_l is the magnetic quantum number whose values range from $-l$ to $+l$. The analytical solution for angle θ is the following polynomial.

$$\Theta(z) = (1-z^2)^{\frac{|m_l|}{2}}\frac{d^{|m_l|}}{dz}P_l(z) \text{ and } z = \cos\theta \tag{42}$$

In Equation 42, P_l(z=cosθ) are solutions to the homogeneous Legendre differential equation given below.

$$\frac{d}{dz}\left[(1-z^2)\frac{dP_l}{dz}\right] + l(l+1)P_l = 0 \text{ (Arfken and Weber, 2005)} \tag{43}$$

Equation 42 instead is the analytical solution to the homogeneous associate Legendre differential equation.

$$\frac{d}{dz}\left[(1-z^2)\frac{d\Theta}{dz}\right]+\left[l(l+1)-\frac{m_l^2}{1-z^2}\right]\Theta=0 \text{ (Arfken and Weber, 2005)} \tag{44}$$

In Equations 43 and 44, $dz{=}-\sin\theta d\theta$ when $z{=}\cos\theta$ involving the angular momentum quantum number l. Empirically, the squared quantized angular momentum is observed (Walker et al., 2014) to be proportional to $l(l{+}1)$ instead of l^2 and this is in correlation with the Heisenbug uncertainty principle of linear momentum.

The major difference between the relativistic Schrödinger differential wave equation and the classical one is in the radial wave function $R(r)$ when taking relativistic effects into account. With reference to the analytical solutions of θ and ϕ (Walker et al., 2014), equation 40 becomes the following differential function of R.

$$-\frac{1}{r^2}\frac{d}{dr}\left(r^2\frac{dR}{dr}\right)+\frac{1}{r^2}l(l+1)R-\left[\frac{E_s^2-m_e^2c^4}{\hbar^2c^2}+\frac{2E_s}{\hbar c}\frac{Z\alpha}{r}+\frac{Z^2\alpha^2}{r^2}\right]R=0 \tag{45}$$

Multiply -1 through Equation 45, take the derivatives with respect to r on the left-hand-side of Equation 45, and substitute $+\left[(E_s^2-m_e^2c^4)/(\hbar^2c^2)\right]$ with equivalent expression $-\left\{-\left[(E_s^2-m_e^2c^4)/(\hbar^2c^2)\right]\right\}$, Equation 45 becomes

$$\frac{2}{r}\frac{dR}{dr}+\frac{d^2R}{dr^2}+\frac{2E_s}{\hbar c}\frac{Z\alpha}{r}R-\left[-\frac{(E_s^2-m_e^2c^4)}{\hbar^2c^2}\right]R+\frac{Z^2\alpha^2-l(l+1)}{r^2}R=0 \tag{46}$$

Then use the following same relationship as in the classical Schrödinger differential wave equation for the unitless parameter ρ (Walker et al., 2014) to have a dimensionless distance variable instead of r.

$$\rho=2\beta r \tag{47}$$

Where β^2 is set equal to next expression for E_s values greater than zero and less than the electron rest mass energy, since the mechanical energy E_m is a negative number greater than the negative rest mass energy value of the electron.

$$\beta^2=-\frac{(E_s^2-m_e^2c^4)}{\hbar^2c^2}=\frac{1}{\hbar^2c^2}(m_e^2c^4-E_s^2)>0 \qquad \text{If } 0<E_s<m_ec^2 \text{ and } -m_ec^2<E_m<0 \tag{48}$$

Note that the units of β is 1/meter. Equation 46 is now transformed into units of ρ since $r=\frac{\rho}{2\beta}$ with the substitution of $\beta^2=-\left[(E_s^2-m_e^2c^4)/(\hbar^2c^2)\right]$ into Equation 46

$$(2\beta)^2\frac{2}{\rho}\frac{dR}{d\rho}+(2\beta)^2\frac{d^2R}{d\rho^2}+(2\beta)^2\frac{1}{\beta}\frac{E_s}{\hbar c}\frac{Z\alpha}{\rho}R-\beta^2R+(2\beta)^2\frac{Z^2\alpha^2-l(l+1)}{\rho^2}R=0 \tag{49}$$

When one applies the following expression for deriving Equation 49.

$$2\beta\frac{2E_s}{\hbar c}=4\beta\frac{\beta}{\beta}\frac{E_s}{\hbar c}=(2\beta)^2\frac{1}{\beta}\frac{E_s}{\hbar c} \tag{50}$$

Again, unitless parameter γ is used to obtain a nonhomogeneous associate Laguerre differential equation as in the case of the classical Schrödinger differential wave equation (Walker et al., 2014), and this time

$$\gamma = \frac{E_s Z\alpha}{\beta\hbar c} = \frac{E_s Z\alpha}{\frac{\sqrt{m_e^2c^4 - E_s^2}\hbar c}{\hbar c}} = \frac{E_s Z\alpha}{\sqrt{m_e^2c^4 - E_s^2}} = \frac{E_s Z\alpha}{m_e c^2\sqrt{1 - E_e^2}} = \frac{E_e Z\alpha}{\sqrt{1 - E_e^2}} \qquad 0 < E_s < m_e c^2 \qquad E_e = \frac{E_s}{m_e c^2} \tag{51}$$

In Equation 51, E_e is in units of the electron rest mass energy. Rearrangement of Equation 51 will yield the following equation with E_s as a positive square root function of γ since $0<E_s<m_e c^2$.

$$E_s = \frac{m_e c^2}{\sqrt{1 + \frac{Z^2\alpha^2}{\gamma^2}}} \text{ or } E_e = \frac{E_s}{m_e c^2} = \frac{1}{\sqrt{1 + \frac{Z^2\alpha^2}{\gamma^2}}} \tag{52}$$

After dividing Equation 49 through by $(2\beta)^2$ and substituting in γ, Equation 49 ends up in a similar form as for the classical Schrödinger differential radial wave equation but with the addition of the $Z^2\alpha^2$ term divided by ρ^2.

$$\frac{2}{\rho}\frac{dR}{d\rho} + \frac{d^2R}{d\rho^2} + \frac{\gamma}{\rho}R - \frac{1}{4}R + \frac{Z^2\alpha^2 - l(l+1)}{\rho^2}R = 0 \tag{53}$$

And again, the analytical solution of Equation 53 will be very similar to the classical Schrödinger differential radial wave equation (Walker et al., 2014) concerning radial function $R(\rho)$, but what will be different is the exponent s in the polynomial $F(\rho)$.

$$R(\rho) = R = e^{-\rho/2}F(\rho) = e^{-\rho/2}F \tag{54}$$

The negative exponential factor in Equation 54 is derived for large values of ρ where the expression in Equation 53 becomes the following approximation.

$$\frac{d^2R}{d\rho^2} - \frac{1}{4}R \approx 0 \left(\text{Analytical solution } R = e^{-\rho/2}.\right) \tag{55}$$

After taking the first and second derivative of Equation 54 with respect to ρ, substituting them into Equation 53, and dividing out $e^{-\rho/2}$

$$\frac{d^2F}{d\rho^2} + \left(\frac{2}{\rho} - 1\right)\frac{dF}{d\rho} + \left(\frac{\gamma - 1}{\rho}\right)F + \frac{Z^2\alpha^2 - l(l+1)}{\rho^2}F = 0 \tag{56}$$

If one multiplies Equation 56 with ρ and then subtract the right-hand term on both sides of this equation, one has the following result which is a nonhomogeneous associate Laguerre differential equation.

$$\rho\frac{d^2F}{d\rho^2} + (2 - \rho)\frac{dF}{d\rho} + (\gamma - 1)F = \frac{l(l+1) - Z^2\alpha^2}{\rho}F \tag{57}$$

The homogenous associate Laguerre differential equation is the following in terms of x and y.

$$x\frac{d^2y}{dx^2} + (\kappa + 1 - x)\frac{dy}{dx} + \eta y = 0 \text{ (Arfken, and Weber, 2005)} \tag{58}$$

In Equation 58, both κ and η are integers with the following analytical series solution and coefficients.

$$y = \sum a_k x^k \qquad a_1 = \frac{-\eta}{\kappa + 1}a_0 \qquad a_{k+1} = \frac{k - \eta}{(k+1)k + (\kappa + 1)(k+1)}a_k \tag{59}$$

Apparently, the series solution in Equation 59 terminates when $k=\eta$. Compared to Equation 59, in Equation 56 $F=y$, $\rho=x$, $\kappa=1$ and $\eta=\gamma-1$.

Therefore, the analytical solution to the function $F(\rho)$ is the following expansion series in powers of ρ, as for the classical Schrödinger differential radial wave equation (Walker et al., 2014), where a constant value s is added to the exponentials of ρ to match with the nonhomogeneous differential equation given in Equation 57.

$$F = \sum_{k=0}^{K} a_k \rho^{s+k} \qquad \frac{dF}{d\rho} = \sum_{k=0}^{K} (s+k) a_k \rho^{s+k-1} \qquad \frac{dF^2}{d\rho^2} = \sum_{k=0}^{K} (s+k)(s+k-1) a_k \rho^{s+k-2} \tag{60}$$

However, this time s will not be equal to angular momentum quantum number l, and $\eta{=}\gamma{-}1$ is a non-integer real number instead of an integer. If one performs the substitutions of the expressions in Equation 60 into Equation 57, one has the following result.

$$\sum_{k=0}^{K} (s+k)(s+k-1) a_k \rho^{s+k-1} + 2\sum_{k=0}^{K} (s+k) a_k \rho^{s+k-1} - \sum_{k=0}^{K} (s+k) a_k \rho^{s+k} + (\gamma-1)\sum_{k=0}^{K} a_k \rho^{s+k} = [l(l+1) - Z^2\alpha^2] \sum_{k=0}^{K} a_k \rho^{s+k-1} \tag{61}$$

Then separate out terms of $k{=}0$ for the two series on the left-hand side of Equation 61, and the same for the $k{=}0$ component of the series on the right-hand side of the equal sign.

$$[s(s-1) + 2s] a_0 \rho^{s-1} + \sum_{k=1}^{K} (s+k)(s+k-1) a_k \rho^{s+k-1} + 2\sum_{k=1}^{K} (s+k) a_k \rho^{s+k-1} - \sum_{k=0}^{K} (s+k) a_k \rho^{s+k} + (\gamma-1)\sum_{k=0}^{K} a_k \rho^{s+k} = [l(l+1) - Z^2\alpha^2] a_0 \rho^{s-1} + [l(l+1) - Z^2\alpha^2] \sum_{k=1}^{K} a_k \rho^{s+k-1} \tag{62}$$

Then reset the series on both sides of Equation 62 for terms ρ^{s+k-1} into ρ^{s+k} by addition of one so to have the initial value of $k{=}0$ instead of $k{=}1$, and collect like terms.

$$s(s+1) a_0 \rho^{s-1} + \sum_{k=0}^{K} [(s+k+1)(s+k) + 2(s+k+1)] a_{k+1} \rho^{s+k} - \sum_{k=0}^{K} (s+k) a_k \rho^{s+k} + (\gamma-1)\sum_{k=0}^{K} a_k \rho^{s+k} = [l(l+1) - Z^2\alpha^2] a_0 \rho^{s-1} + [l(l+1) - Z^2\alpha^2] \sum_{k=0}^{K} a_{k+1} \rho^{s+k} \tag{63}$$

In Equation 63 it is possible to evaluate s since a_0 cannot be equal to zero.

$$s(s+1) = l(l+1) - Z^2\alpha^2 \quad \text{or} \quad s^2 + s + [Z^2\alpha^2 - l(l+1)] = 0 \tag{64}$$

The quadratic formula below is used to evaluate s.

$$s = \frac{-1 \pm \sqrt{1^2 + 4[l(l+1) - Z^2\alpha^2]}}{2} = -\frac{1}{2} \pm \sqrt{\frac{1}{4} + l^2 + l - Z^2\alpha^2} = -\frac{1}{2} \pm \sqrt{\left(l + \frac{1}{2}\right)^2 - Z^2\alpha^2} \tag{65}$$

Next, the following part of Equation 63 is rearranged and set equal to zero so to be able to evaluate γ.

$$\sum_{k=0}^{K} \{(s+k+1)(s+k) + 2(s+k+1) + [Z^2\alpha^2 - l(l+1)]\} a_{k+1} \rho^{s+k} + \sum_{k=0}^{K} [(\gamma-1) - (s+k)] a_k \rho^{s+k} = 0 \tag{66}$$

Thus, one has the following relationship between coefficients a_k and a_{k+1} from Equation 66 above

$$a_{k+1} = \frac{(s+k) - (\gamma-1)}{(s+k+1)(s+k) + 2(s+k+1) + [Z^2\alpha^2 - l(l+1)]} a_k \tag{67}$$

And the series terminates when the numerator in Equation 67 is equal to zero. Hence, γ is the following function in Equation 68 below noting that addition instead of subtraction in the analytical solution given in Equation 65 is utilized, since theoretically a quantum number of any orbital must be positive and greater than zero in value.

$$\gamma = s + k + 1 = -\frac{1}{2} + \sqrt{\left(l+\frac{1}{2}\right)^2 - Z^2\alpha^2} + (n-l) = n - \left(l+\frac{1}{2}\right) + \sqrt{\left(l+\frac{1}{2}\right)^2 - Z^2\alpha^2} > 0 \tag{68}$$

The $k{+}1{=}n{-}l$, as in the classical Schrödinger differential wave equation (Walker et al., 2014), mandates that $l_{max}{=}n{-}1$. Angular momentum quantum number l is less than the principal quantum number n. Substituting addition in Equation 65 for s and Equation 68 for γ, Equation 67 becomes the next expression.

$$a_{k+1} = \frac{k+l+1-n}{2(k+1)\left[\sqrt{\left(l+\frac{1}{2}\right)^2 - Z^2\alpha^2}\right] + k^2 + 2k + 1} a_k \tag{69}$$

Another important fact is that values of γ for the $1s$ orbitals of all 118 elements on the current Periodic Table of Elements, beyond copper to element 118 (oganesson), are estimated to be greater than 1/2.

Two Problems of the Relativistic Schrödinger Differential Wave Equation for $l{=}0$ Quantum Levels

There are two problems with the relativistic version of the Schrödinger differential wave equation for quantum levels with angular momentum quantum number $l{=}0$. With regard to the first problem, the value E_e in units of the electron rest mass energy, calculated from the measured $1s$ ionization energy of Cu^{28+} (Table III) (Wikipedia: The Free Encyclopedia, 2025), is 0.9773612, greater than the theoretical value 0.9762209 evaluated by the analytical solution of the relativistic Schrödinger differential wave equation. Using Equation 68 to determine the value of γ for Cu^{28+} hydrogen-like cation containing 29 protons in the copper nucleus with the single electron in the $1s$ orbital

$$\gamma = n - \left(l+\frac{1}{2}\right) + \sqrt{\left(l+\frac{1}{2}\right)^2 - Z^2\alpha^2} = 1 - \left(0+\frac{1}{2}\right) + \sqrt{\left(0+\frac{1}{2}\right)^2 - 29^2\frac{1}{137.036^2}} = 0.9530073 \tag{70}$$

And using this value of γ from Equation 70 in Equation 52 yields the following theoretical E_e value for the $1s$ ionization energy in a Cu^{28+} hydrogen-like cation.

$$E_e = \frac{E_s}{m_e c^2} = \frac{1}{\sqrt{1+\frac{Z^2\alpha^2}{\gamma^2}}} = \frac{1}{\sqrt{1+\frac{29^2\left(\frac{1}{137.036}\right)^2}{0.9530073^2}}} = 0.9762209 \tag{71}$$

However, if one uses the measured $1s$ ionization energy IE for Cu^{28+} (Table III), experimental E_e is greater than the number calculated in Equation 71.

$$E_{e,Exp} = 1 - \frac{IE}{N_A}\frac{1}{m_e c^2} = 1 - \frac{1{,}116{,}105{,}000\ \text{Joules}}{6.022141\times10^{23}}\frac{1}{9.10938\times10^{-31}\text{kg}(299782458\ \text{m/s})^2} = 0.9773612 \tag{72}$$

Table III Measured Ionization Energies for the $1s$ Electron in Hydrogen and Hydrogen-Like Cations

Atomic Number	Element	Cation	Measured $1s$ Ionization Energy (kJ/mole)
1	Hydrogen	H	1,312.0
2	Helium	He^{+}	5,250.5
3	Lithium	Li^{2+}	11,815.0
4	Beryllium	Be^{3+}	21,006.6
5	Boron	B^{4+}	32,826.17
6	Carbon	C^{5+}	47,277.0
7	Nitrogen	N^{6+}	64,360.
8	Oxygen	O^{7+}	84,078.0
9	Fluorine	F^{8+}	106,434.3
10	Neon	Ne^{9+}	131,432
11	Sodium	Na^{10+}	159,076
12	Magnesium	Mg^{11+}	189,368
13	Aluminum	Al^{12+}	222,316
14	Silicon	Si^{13+}	257,923
15	Phosphorus	P^{14+}	296,195
16	Sulfur	S^{15+}	337,138
17	Chlorine	Cl^{16+}	380,760
18	Argon	Ar^{17+}	427,066
19	Potassium	K^{18+}	476,063
20	Calcium	Ca^{19+}	572,762
21	Scandium	Sc^{20+}	582,163
22	Titanium	Ti^{21+}	639,294
23	Vanadium	V^{22+}	699,144
24	Chromium	Cr^{23+}	761,733
25	Manganese	Mn^{24+}	827,067
26	Iron	Fe^{25+}	895,161
27	Cobalt	Co^{26+}	966,023
28	Nickel	Ni^{27+}	1,039,668
29	Copper	Cu^{28+}	1,116,105

In Equation 72, the numerical value of Avogadro's number N_A (Miessler et al., 2014) is in the denominator since ionization energies are normally given in units of kilojoules per mole. The calculated E_e in Equation 72 from measured data is greater than the result in Equation 71, showing that the theoretical value overestimates the actual ionization energy. Concerning the second problem, this appears in Equations 65 and 68 for the hydrogen-like cation Tm^{68+} when the angular momentum quantum number l=0. For the Tm^{68+} hydrogen-like cation, evaluation of s and γ using Equations 65 and 68 both yield a complex number.

$$\gamma = n - \left(0 + \frac{1}{2}\right) + \sqrt{\left(0 + \frac{1}{2}\right)^2 - 69^2 \frac{1}{137.036000^2}} = n - \frac{1}{2} + \sqrt{\frac{1}{4} - 69^2 \frac{1}{137.036000^2}} = n - \frac{1}{2} + i0.0594112 \quad (73)$$

To evaluate a numerical solution which matches experimental $1s$ ionization energy value for hydrogen-like cation Cu^{28+}, first compute γ_{Exp} from evaluated $E_{e,Exp}$ of Equation 72 after rearrangement of Equation 52 to separate out γ_{Exp}.

$$\gamma_{Exp} = E_{e,Exp} \frac{Z\alpha}{\sqrt{1 - E_{e,Exp}^2}} \tag{74}$$

Since there is no analytical solution that matches measurement, a numerical solution is necessary. As such, we first inserted the calculated value of γ_{Exp} from Equation 74 into Equation 53 and performed a numerical analysis of the radial differential wave equation using the finite-difference technique (LeVeque, 2017). This was performed by using Microsoft Excel (Microsoft, 2018) for the following expression:

$$\frac{2}{\rho}\frac{dR}{d\rho} + \frac{d^2R}{d\rho^2} + \frac{\gamma_{Exp}}{\rho}R - \frac{1}{4}R + \frac{Z^2\alpha^2 - l(l+1)}{\rho^2}R = 0 \tag{75}$$

After performing the next four steps, Equation 75 becomes the numerical expression in Equation 79 for the finite-difference technique used to perform a numerical integration.

In Step 1, use the following approximation in Equation 76 below for first and second derivatives with respect to ρ while using the calculated γ_{Exp} from experimentally measured ionization energy.

$$\frac{2}{\rho_{i+1}}\frac{R_{i+1} - R_i}{\Delta\rho} + \frac{\frac{R_{i+2} - R_{i+1}}{\Delta\rho} - \frac{R_{i+1} - R_i}{\Delta\rho}}{\Delta\rho} + \left[\frac{\gamma_{Exp}}{\rho_{i+1}} + \frac{Z^2\alpha^2 - l(l+1)}{\rho_{i+1}^2} - \frac{1}{4}\right]R_{i+1} = 0 \tag{76}$$

In Step 2, note that the approximate second derivative with respect to ρ is simplified to the ratio on the left-hand-side of Equation 77 given below.

$$\frac{R_{i+2} - 2R_{i+1} + R_i}{\Delta\rho^2} + \frac{2}{\rho_{i+1}}\left(\frac{R_{i+1} - R_i}{\Delta\rho}\right) + \left[\frac{\gamma_{Exp}}{\rho_{i+1}} + \frac{Z^2\alpha^2 - l(l+1)}{\rho_{i+1}^2} - \frac{1}{4}\right]R_{i+1} = 0 \tag{77}$$

For Step 3, collect all like terms in Equation 77 to arrive at the next expression.

$$\frac{R_{i+2}}{\Delta\rho^2} + \frac{R_i - 2R_{i+1}}{\Delta\rho^2} + \frac{2}{\rho_{i+1}}\left(\frac{R_{i+1} - R_i}{\Delta\rho}\right) + \left[\frac{\gamma_{Exp}}{\rho_{i+1}} + \frac{Z^2\alpha^2 - l(l+1)}{\rho_{i+1}^2} - \frac{1}{4}\right]R_{i+1} = 0 \tag{78}$$

Afterwards, finally in Step 4 separate out the newly calculated R_{i+2} value in Equation 79 as shown below.

$$R_{i+2} = 2R_{i+1} - R_i + \Delta\rho\frac{2}{\rho_{i+1}}(R_i - R_{i+1}) + \Delta\rho^2\left[\frac{1}{4} + \frac{l(l+1) - Z^2\alpha^2}{\rho_{i+1}^2} - \frac{\gamma_{Exp}}{\rho_{i+1}}\right]R_{i+1} \tag{79}$$

Then using the values of ρ_{i+1}, R_i, and R_{i+1} with $\Delta\rho$ value set equal to either +0.001 or −0.001, depending upon the direction in the ρ-axis taken, to calculate the new value of R_{i+2} in Equation 79.

For the 1s and other ns orbitals with angular momentum quantum number l=0, the following modification of Equation 79 was found to be necessary by adding constant σ-parameter to dimensionless ρ when using the experimental value of γ_{Exp} evaluated from measured $1s$ ionization energies of hydrogen-like cations.

$$R_{i+2} = 2R_{i+1} - R_i + \Delta\rho\frac{2}{\rho_{i+1}}(R_i - R_{i+1}) + \Delta\rho^2\left[\frac{1}{4} - \frac{Z^2\alpha^2}{(\rho_{i+1} + \sigma)^2} - \frac{\gamma_{Exp}}{(\rho_{i+1} + \sigma)}\right]R_{i+1} \tag{80}$$

Without this modification, the numerical plot of R as a function of ρ decreases in value within short distances from the atomic nucleus (Figure 1), resulting in a negative minimum value at the center

of the atomic nucleus rather than a positive maximum value. It is obvious that the small definite volume of the atomic nucleus, as well as that of the electron, is modeled by the insertion of a constant σ-parameter. This constant σ-parameter is set equal to an evaluated constant C equal to 3.71, such that σ is equal to 3.71 times an estimated nuclear radius (Table IV). A logarithmic plot of Figure 2 was utilized in estimating the value of the constant C where near the estimated copper nucleus radius the logarithmic plot becomes nonlinear and increases to a maximum value at the center of the atomic nucleus. In units of meters, the nuclear radius is estimated (Wong, 1998) as 1.2×10^{-15} times the atomic mass number A raised to the one-third power ($r_{nucl}=1.2\times10^{-15}A^{1/3}$ meter), but instead for copper, the atomic weight listed on the Periodic Table of Elements is used for estimating the radius of the copper nucleus due to two naturally occurring copper isotopes. Then, the calculation of $\sigma=C(2\beta\times r_{nucl})$ is employed to convert the value of σ-parameter from meters into the dimensionless ρ. The negative value of $\Delta\rho=-0.001$ is used instead of $+0.001$ since the maximum value of R is unknown at the center of the atomic nucleus. One can initially set R_1 to a very small value slightly greater than or slightly less than zero at $\rho_1\geq25.000$, initial value of ρ_1 dependent upon the ns orbital size, and then set the value of R_2 to a very small number slightly greater than or slightly less than R_1, depending upon the shape of the radial wave function, at $\rho_2=\rho_1+\Delta\rho$. The initial values of R_1 and R_2 are adjusted to have a normalized numerical plot of $R(\rho)$ and a continuous numerical solution for $F(\rho)$. Afterwards, finish off evaluation of the radial wave function R using Equation 80, rather than Equation 79, consistently up to $\rho_{i+2}=0$ at the center-of-mass of the atomic nucleus. Figure 2 displays the normalized numerical evaluation of the radial wave function for the $1s$ electron in the Cu^{28+} hydrogen-like cation using the measured ionization energy of the $1s$ orbital and the inclusion of the σ-parameter. The maximum value at the center of the atomic nucleus at $\rho=0$ is a positive number. With the inclusion of the σ-parameter, the differential expression in Equation 75 becomes a differential equation with no known analytical solution and only a numerical solution is possible using finite-difference technique with initial boundary conditions. Thus, measured data is required along with a numerical solution via the finite-difference technique. In addition, to obtain the smooth shape of the numerical integration at the center of the atomic nucleus ($\rho=0$), the value of the constant C is varied to determine the most appropriate value of the σ-parameter in Equation 80.

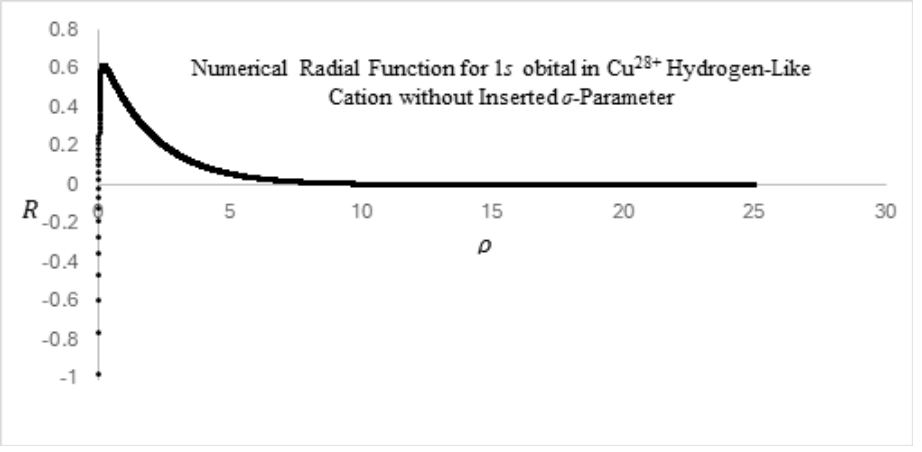

Figure 1 Normalized numerically calculated radial function R for the $1s$ orbital in the Cu^{28+} hydrogen-like cation with $\gamma_{Exp}=0.9775719$, factor $f_{exp}=0.489570$, and $E_{e,Exp}=0.9773612$. For the x-axis $r=0.912571\ \rho$ in units of picometers (10^{-12} meters).

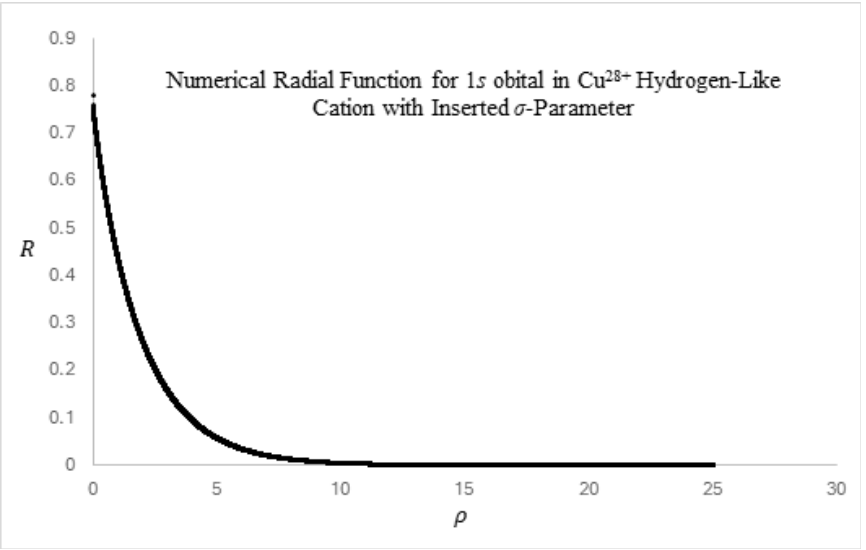

Figure 2 Normalized numerically calculated radial function R for the $1s$ orbital in the Cu^{28+} hydrogen-like cation with γ_{Exp}=0.9775719, factor f_{exp}=0.489570, and $E_{e,Exp}$=0.9773612. For the x-axis r=0.912571 ρ in units of picometers (10^{-12} meter) and σ=0.0195 in units of ρ.

Table IV Evaluated σ-Parameters for the Cu28+ Hydrogen-Like Cation in Unitless and Picometers

$\sigma = C2\beta \times r_{nucl} = C2\beta \times 1.2AW^{1/3} = C2\beta \times 1.2 \times 63.5^{1/3} = C2\beta \times 4.79$ femtometer (10^{-15} meter)
β given in units of 1/picometers and 1 picometer = 10^{-12} meter

Orbital	β (1/pm)	Constant C	r_{nucl} in unitless ρ	σ-Parameter in unitless ρ
$1s$	0.548	3.71	0.00525	0.0195
$2s$	0.276	3.71	0.00264	0.00979
$3s$	0.184	3.71	0.00176	0.00653
$4s$	0.138	3.71	0.00132	0.00490
$5s$	0.110	3.71	0.00105	0.00390
$6s$	0.0916	3.71	0.000877	0.00325
$7s$	0.0785	3.71	0.000752	0.00279

In addition, one can evaluate an experimental factor f_{exp} in Equation 81 below, by the calculated γ_{Exp} when using measured ionization energies of $1s$ electron in hydrogen-like cations for principal quantum number n=1 and angular momentum quantum number l=0.

$$\gamma_{Exp} = 1 - \left(0 + \frac{1}{2}\right) + \sqrt{\left(0 + \frac{1}{2}\right)^2 - f_{Exp} Z^2 \alpha^2} \tag{81}$$

Such that after separating out the factor f_{exp} in Equation 81, one has the following expression.

$$f_{Exp} = \frac{\gamma_{Exp} - \gamma_{Exp}^2}{Z^2\alpha^2} \tag{82}$$

If one assumes that the value of factor f_{exp} does not change with principal quantum number n, radial functions for larger values of the principal quantum number n with angular momentum quantum number l=0 can be determined numerically. However, it will again be necessary to insert the σ-parameter in Equation 80 to obtain continuous plots of both $R(\rho)$ and $F(\rho)$. Figure 3 displays the normalized numerical radial wave function of the $2s$ electron in the Cu^{28+} cation which has a higher energy value, and Table IV displays the evaluated σ-parameters for the $1s$ to $7s$ orbitals in both unitless parameter ρ and a constant value in femtometers (10^{-15} meters) for the estimated radius of a copper nucleus. For all the ns orbitals analyzed, the evaluated σ-parameters are displayed at three significant figures. In the numerical integration of Figure 3, the evaluated factor f_{exp} in Equation 82, from the measured ionization energy of the $1s$ hydrogen-like cation Cu^{28+}, is used again by insertion in Equation 83 below for principal quantum number n=2 and angular momentum quantum number l=0.

$$\gamma_{ns} = n - \left(0 + \frac{1}{2}\right) + \sqrt{\left(0 + \frac{1}{2}\right)^2 - f_{Exp}Z^2\alpha^2} \text{ and } E_s = \frac{m_e c^2}{\sqrt{1 + \frac{Z^2\alpha^2}{\gamma_{ns}^2}}} \tag{83}$$

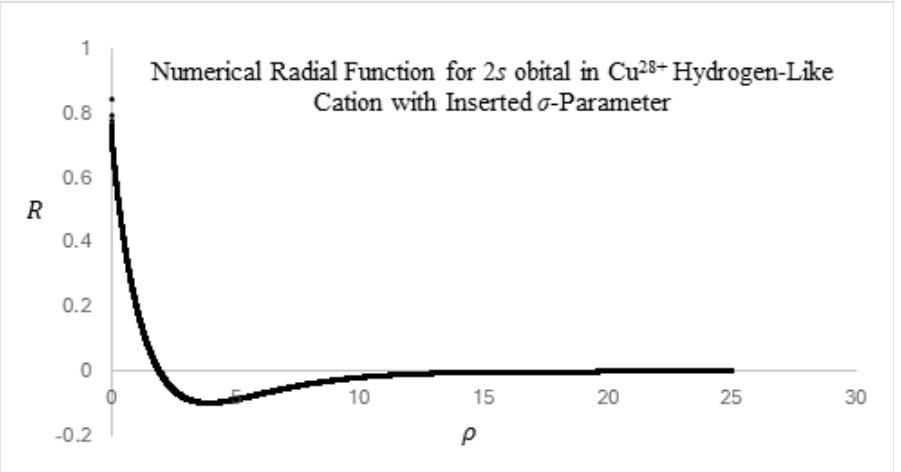

Figure 3 Normalized numerically calculated radial function R for the $2s$ orbital in the Cu^{28+} hydrogen-like cation using factor f_{exp}=0.489570 and γ_{ns}=1.977572, resulting in E_e=0.9943230>0.9773612. For the x-axis r=1.814588 ρ in units of picometers (10^{-12} meter) and σ=0.00979 in units of ρ.

This computed value of γ_{ns} is then used to calculate the energy level by Equation 52, and γ_{ns} is then inserted into Equation 80 to perform the numerical result with inclusion with the σ-parameter. Note that the radial wave function plot of the $2s$ electron in Figure 3 has a single node.

Theoretically, the ns electrons pass through the atomic nucleus in classical oscillations because there is zero angular momentum of the electron in an atomic orbital that has the angular momentum quantum number l=0. In classical physics (Walker et al., 2014), the electron inside the atomic nucleus will experience a Coulomb force matching that of the classical harmonic oscillator if the positive charge density of the atomic nucleus is constant, similar to an object falling through a linear hole through the center of a planet for the force of gravity. It is important to note that subatomic particles and the atomic nucleus as well are not point masses. Theoretically the electron, proton, and neutron are spherical in shape. The radius of the proton and neutron are estimated to be as small as 1 femtometer (10^{-15} meters). Since the electron has a rest mass value nearly 1,800 times less than that of a proton or neutron, the radius of the electron is around 10^{-17} meter assuming the electron has the same density as the proton or neutron. This may be the physical origin of the required σ-parameter for a numerical solution with lower ionization energy values as compared to the analytical solution of the relativistic Schrödinger differential wave equation.

Yet, it is important to note that the evaluated σ-parameter using experimental ionization energy is slightly more than twice the estimated radius of the nucleus or diameter. If one inserts the estimated radius of the atomic nucleus, the numerical value of the factor "f_{ns}" ends up lesser in value than the experimental value f_{Exp} and the calculated ionization energy will be larger in value than observed experimentally. Since the differential expression in Equation 75 with the addition of the σ-parameter in the denominator has no analytical solution and only a numerical one, it is necessary, therefore, to use experimental data in obtaining the most appropriate value of the σ-parameter. Again, due to the wave-particle duality of the electron and the atomic nucleus, this may help to explain why the σ-parameter is larger than the estimated diameter of the atomic nucleus.

.

The Relativistic Schrödinger Differential Wave Equation for l>0 Quantum Levels

When numerically displaying normalized radial wave functions for angular momentum quantum numbers greater than zero, l>0, the differential is $\Delta\rho$=+0.001, positive value since at ρ_1=0, R_1=0. Theoretically, electrons with angular momentum l>0 are exterior of the atomic nucleus due to having quantized value of angular momentum greater than zero. Initial value of R_2 at ρ_2=0.001 is set equal to a very small number slightly greater than zero, such that a normalized numerical plot for $R(\rho)$ is the result. When accomplishing a numerical plot for the radial wave function of angular momentum quantum number greater than zero l>0, a varied factor f_{nl} can be inserted into Equation 68

$$\gamma_{nl} = n - \left(l + \frac{1}{2}\right) + \sqrt{\left(l + \frac{1}{2}\right)^2 - f_{nl} Z^2 \alpha^2} \text{ and } E_s = \frac{m_e c^2}{\sqrt{1 + \frac{Z^2\alpha^2}{\gamma_{nl}^2}}} \tag{84}$$

This calculated value γ_{nl} can then be placed into Equation 79 instead of Equation 80 to conduct a numerical plot with no added σ-parameter (σ=0). The factor f_{nl} is varied until the numerical plot of R approaches zero at $\rho \geq 25.000$ without any divergences, along with the numerical plot of function $F(\rho)$ being continuous. Afterwards, the final value of γ_{nl} is determined by Equation 84 from the varied factor f_{nl}, and this final value γ_{nl} is used to calculate the energy level E_s by Equation 52. The factor

f_{nl} values observed are all slightly greater than one (Table V), showing that the analytical solution is appropriate for quantum states that have angular momentum quantum number l=1,2,3,... It is very likely that numerical error is the result of the factor f_{nl} being slightly greater than one. Yet, in the numerical analysis for l>0 orbitals, one can set factor f_{nl}=1 and vary the σ-parameter in Equation 80 instead to obtain similar results (Table V). This alternative version of numerical integration resulted in σ-parameter values less than the estimated nuclear radius or equal to zero. The requirement of inserting the parameter σ, for some of the orbitals with angular momentum quantum l>0, is again due to the small quantity of error in a numerical integration when using the finite-difference technique. The quantum energy E_s calculated from γ_{nl} values for factor f_{nl}=1 are nearly equal in value with ones for values of f_{nl} slightly greater than one (Table V).

Table V Evaluated f_{nl} Values with σ=0, Determined σ values for f_{nl}=1 for l>0 for Orbitals from $2p$ to $7p$ for Hydrogen-Like cation Cu^{28+}, and Calculated Energy Levels in Units of Electron Rest Mass Energy. Also, listed energy values do not include spin-orbit **S·L** coupling.

Orbital	f_{nl} ($\sigma = 0$)	Energy E_e	σ in unitless ρ ($f_{ln} = 1$)	Energy E_e
$2p$	1.005583	0.9943645	0.000122	0.9943650
$3p$	1.017	0.9974959	0.000245	0.9974963
$3d$	1.0056	0.9975063	0.0000875	0.9975064
$4p$	1.017	0.9985927	0.000236	0.9985929
$4d$	1.008	0.9985971	0.000131	0.9985971
$4f$	1.008	0.9985989	0.000131	0.9985989
$5p$	1.017	0.9991000	0.000252	0.9991001
$5d$	1.008	0.9991023	0.000000	0.9991023
$5f$	1.008	0.9991032	0.000105	0.9991032
$6p$	1.017	0.9993754	0.000000	0.9993755
$6d$	1.008	0.9993767	0.000000	0.9993767
$7p$	1.017	0.9995413	0.000000	0.9995414

Figure 4 displays the numerical plot of the $2p$ orbital using the analytical solution for f_{nl}=1 with the very small value of the σ-parameter equal to 0.000122 in dimensionless distance ρ with an atomic nucleus radius estimated to be 0.00263 in dimensionless distance ρ. Also, one of the energy values for the $2p$ quantum level, $2p_{3/2}$, is slightly higher in energy than the $2s$, but the other one, $2p_{1/2}$, is slightly less (Table VI), referred to as the Lamb shift (Lamb and Retherford, 1947), when taking spin-orbit **S·L** coupling into account between the electron and atomic nucleus. Thus, relativistic effects explain why quantum levels at the same principal quantum number n, but different angular quantum number l, have slightly different energy values. Larger values of the angular momentum quantum number l results in slightly higher energy if spin-orbit **S·L** coupling is not taken into consideration. In the classical Schrödinger differential wave equation (Walker et al., 2014), quantum levels with the same principal quantum number n and different angular momentum quantum number l are equal in energy and thus degenerate when not including spin-orbit **S·L** coupling.

Table VI Energy Levels: Relativistic Schrödinger and Dirac Differential Wave Equations, including Classical Schrödinger, for Cu^{28+} Cation which Incorporate Spin-Orbit **S·L** Coupling for Orbitals $1s$ to $4f$

Energy values are given in units of the rest mass energy of the electron, and the numerical solutions of the relativistic Schrödinger differential wave equation used for listed energy values with listed factor f_{nl}

Spin Level	Relativistic Schrödinger	Factor f_{Exp} and f_{nl}	Relativistic Dirac[1]	Classical Schrödinger[2]
$1s\ (j=0+\frac{1}{2})(l=0)$	0.9773612	0.489570	0.9773513	0.9776078
$2s\ (j=0+\frac{1}{2})(l=0)$	0.9943230	0.489570	0.9943217	0.9944020
$2p$ (No $\mathbf{S}\cdot\mathbf{L}$ coupling)$(l=1)$	0.9943650	1[3]		0.9944020
$2p_{1/2}\ (j=1-\frac{1}{2})(l=1)$	0.9943216	1	0.9943217	0.9943602
$2p_{3/2}\ (j=1+\frac{1}{2})(l=1)$	0.9943867	1	0.9943862	0.9944228
$3s\ (j=0+\frac{1}{2})(l=0)$	0.9974839	0.489570	0.9974835	0.9975120
$3p$ (No $\mathbf{S}\cdot\mathbf{L}$ coupling)$(l=1)$	0.9974963	1		0.9975120
$3p_{1/2}\ (j=1-\frac{1}{2})(l=1)$	0.9974834	1	0.9974835	0.9975058
$3p_{3/2}\ (j=1+\frac{1}{2})(l=1)$	0.9975028	1	0.9975026	0.9975151
$3d$ (No $\mathbf{S}\cdot\mathbf{L}$ coupling)$(l=2)$	0.9975064	1		0.9975120
$3d_{3/2}\ (j=2-\frac{1}{2})(l=2)$	0.9975026	1	0.9975026	0.9975083[2]
$3d_{5/2}\ (j=2+\frac{1}{2})(l=2)$	0.9975089	1	0.9975089	0.9975145
$4s\ (j=0+\frac{1}{2})\ (l=0)$	0.9985877	0.489570	0.9985875	0.9986005
$4p$ (No $\mathbf{S}\cdot\mathbf{L}$ coupling)$(l=1)$	0.9985929	1		0.9986005
$4p_{1/2}\ (j=1-\frac{1}{2})(l=1)$	0.9985875	1	0.9985875	0.9985953
$4p_{3/2}\ (j=1+\frac{1}{2})(l=1)$	0.9985956	1	0.9985956	0.9986031
$4d$ (No $\mathbf{S}\cdot\mathbf{L}$ coupling)$(l=2)$	0.9985971	1		0.9986005
$4d_{3/2}\ (j=2-\frac{1}{2})(l=2)$	0.9985956	1	0.9985956	0.9985989[2]
$4d_{5/2}\ (j=2+\frac{1}{2})(l=2)$	0.9985982	1	0.9985982	0.9986015
$4f$ (No $\mathbf{S}\cdot\mathbf{L}$ coupling)$(l=3)$	0.9985989	1		0.9986005
$4f_{5/2}\ (j=3-\frac{1}{2})(l=3)$	0.9985982	1	0.9985982	0.9985997[2]
$4f_{7/2}\ (j=3+\frac{1}{2})(l=3)$	0.9985995	1	0.9985995	0.9986010

[1]The Dirac relativistic differential wave equation involving 4×4 Puli spin matrices take **S·L** coupling into account, so there are no energy values for "No **S·L** coupling" in the solutions of the Dirac version.

[2]For the classical Schrodinger differential wave equation, there is a problem with inclusion of **S·L** coupling. The evaluated energy value of the $3d_{3/2}$ is less than for the $3s$, and the energy values of the $4d_{3/2}$ and $4f_{5/2}$ is less than that for the $4s$. This is in contradiction to what is observed experimentally.

[3]For angular momentum quantum number $l>0$, the analytical solution of the relativistic Schrödinger differential wave equation will not result in complex number for γ until the number of protons is greater than 205 for angular quantum number $l=1$, greater than 342 for quantum number $l=2$, and greater than 479 for quantum number $l=3$. Thus, one can assume that factor $f_{nl}=1$ unlike the situation for $l=0$ where it is necessary to evaluate the factor f_{Exp}.

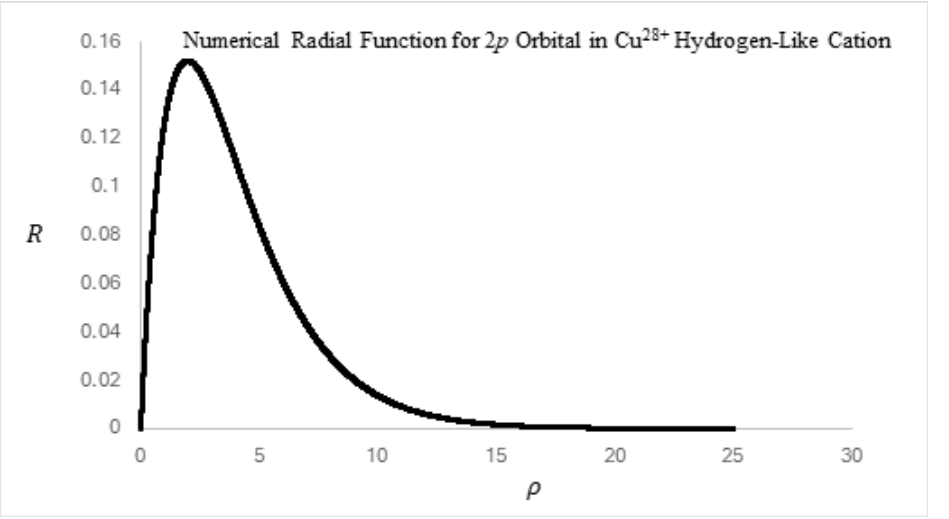

Figure 4 Normalized numerically calculated radial function R for the $2p$ orbital in the Cu^{28+} hydrogen-like cation using factor $f_{nl}=1$ and $\gamma_{nl}=1.984997$, resulting in $E_n=0.9943650>0.9943230$. For the x-axis $r=1.821324$ ρ in units of picometers (10^{-12} meter), and in units of ρ $\sigma=0.000122<r_{nucl}=0.00263$.

Since the analytical solutions for the relativistic Schrödinger equation are quite complex (Table VII), a normalized numerical solution is less tedious and nearly correct. The analytical solution involves gamma-functions of real, non-integer values $\Gamma(s+k)$ since s is equal to non-integer value by Equation 65, that result in irrational numbers evaluated numerically. The classical Schrödinger differential wave equation has gamma-functions of integers $l+k$, involving the angular momentum quantum number, such that $\Gamma(l+k)=(l+k-1)!$, and less complicated negative exponential in the radial wave function. Concerning quantum levels that have the angular momentum number $l=1$, the square root functions in Equations 65 and 68 will not involve negative numbers unless the number of protons is greater than 205.

$$\left(1+\frac{1}{2}\right)^2 - Z^2\alpha^2 = 0 \text{ or } Z = \frac{3/2}{\alpha} = \frac{3}{2} \times 137.036000 = 205.554 \tag{85}$$

With present day technology, element 118, oganesson, is the upper limit possible (Cook, 2010) for producing larger nuclei. From an engineering perspective, it may be impossible as well as physically impossible to produce a radioactive nucleus that has 206 protons due to the physics of the atomic nucleus. In addition, from extrapolation of the experimental data plotted in Figure 5, calculated using the measured data in Table III, one can estimate radial wave functions for hydrogen-like cations beyond copper up to element 118. From the extrapolation of data in Figure 5, element 118 as hydrogen-like cation Og^{117+} is estimated to have an $1s$ ionization energy $E_e=0.546868$ in units of the electron rest mass energy with $\gamma_{exp}=0.562458>1/2$ and factor $f_{exp}=0.331906$.

Table VII Coefficients as Functions of Atomic Number Z for the Analytical Solutions to the Relativistic Schrödinger Differential Wave Equation for $l > 0$ Series Expansion Exponents $k = 1$ to $k = 4$ for $\gamma > \frac{1}{2}$ so $a_{k+1} = \frac{k+l+1-n}{2(k+1)\left[\sqrt{\left(l+\frac{1}{2}\right)^2 - Z^2\alpha^2}\right] + k^2 + 2k + 1} a_k$

Value of k	
1	$a_1 = \frac{1+l-n}{2\sqrt{\left(l+\frac{1}{2}\right)^2 - Z^2\alpha^2}+1} a_0$
2	$a_2 = \left[\frac{2+l-n}{4\sqrt{\left(l+\frac{1}{2}\right)^2 - Z^2\alpha^2}+4}\right]\left[\frac{\mathbf{1+l-n}}{2\sqrt{\left(l+\frac{1}{2}\right)^2 - Z^2\alpha^2}+1}\right] a_0$
3	$a_3 = \left[\frac{3+l-n}{6\sqrt{\left(l+\frac{1}{2}\right)^2 - Z^2\alpha^2}+9}\right]\left[\frac{2+l-n}{4\sqrt{\left(l+\frac{1}{2}\right)^2 - Z^2\alpha^2}+4}\right]\left[\frac{\mathbf{1+l-n}}{2\sqrt{\left(l+\frac{1}{2}\right)^2 - Z^2\alpha^2}+1}\right] a_0$
4	$a_4 = \left[\frac{4+l-n}{8\sqrt{\left(l+\frac{1}{2}\right)^2 - Z^2\alpha^2}+16}\right]\left[\frac{3+l-n}{6\sqrt{\left(l+\frac{1}{2}\right)^2 - Z^2\alpha^2}+9}\right]\left[\frac{2+l-n}{4\sqrt{\left(l+\frac{1}{2}\right)^2 - Z^2\alpha^2}+4}\right]\left[\frac{\mathbf{1+l-n}}{2\sqrt{\left(l+\frac{1}{2}\right)^2 - Z^2\alpha^2}+1}\right] a_0$

Exponential Function and Exponential in Series for $0 < E_s < m_e c^2$

Exponential Function $e^{-\rho/2} = e^{\frac{-\sqrt{m_e^2c^2 - E_s^2}}{\hbar c} r}$

Exponential in Series $\rho^{s+k} = \rho^{\left[-\frac{1}{2}+\sqrt{\left(l+\frac{1}{2}\right)^2 - Z^2\alpha^2}\right]+k} = \left(\frac{2}{\hbar c}\sqrt{m_e^2c^2 - E_s^2}\, r\right)^{\left[-\frac{1}{2}+\sqrt{\left(l+\frac{1}{2}\right)^2 - Z^2\alpha^2}\right]+k}$

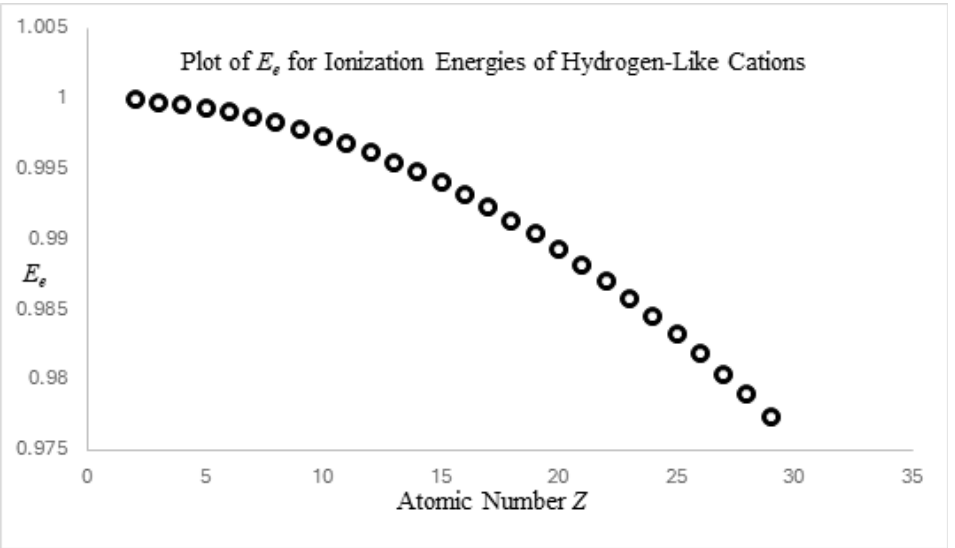

Figure 5 Plot of ionization energies E_e of hydrogen-like cations from He^+ to $Cu2^{8+}$ with respect to the rest mass energy of the electron $m_e c^2$. Black filled circles are from measured data and the white circles are from the following polynomial fit to the data.

$$E_e = 1 - (8.63884\times10^{-13}Z^5 + 3.23529\times10^{-10}Z^4 - 5.80965\times10^{-11}Z^3 + 2.66259\times10^{-5}Z^2 - 2.19743\times10^{-9}Z)$$

Spin-Orbit S·L Coupling for the Relativistic Schrödinger Differential Wave Equation

The orbiting electron in the atom experiences a magnetic field **B** from the positively charged atomic nucleus. Relative to the electron, the atomic nucleus is orbiting in the opposite direction producing this magnetic field. Thus, there is the following torque **τ** experienced by the electron which has the magnetic dipole $\boldsymbol{\mu}_s$ due to the intrinsic spin of the negatively charged electron.

$$\boldsymbol{\tau} = \boldsymbol{\mu}_s \times \mathbf{B} = \left(-\frac{g_s \mu_b}{\hbar}\right)\mathbf{S} \times \mathbf{B} \text{ (Walker et al., 2014)} \tag{86}$$

Concerning this torque in Equation 86, **S** is the angular momentum vector for the intrinsic spin of $1/2$ of the electron. Also, $\mu_b = \frac{q\hbar}{2m_e}$ in Equation 86 is the Bohr magnetron for the electron, and g_s=2 as determined by experimental results in the Stern-Gerlach experiment (Walker et al., 2014). The negative sign for the magnetic dipole $\boldsymbol{\mu}_s$ arises from the negative charge of the electron. Below in Equation 87, the mathematical expression of this magnetic field **B** is shown as derived by the Biot-Savart Law (Walker et al., 2014) since the tangential velocity is $-\mathbf{v}$ of the atomic nucleus relative to the electron tangential velocity **v** in the opposite direction.

$$\mathbf{B} = -\frac{\mu_0 Zq}{4\pi}\frac{\mathbf{v}\times\mathbf{r}}{r^3} = -\varepsilon_0\mu_0\left(\frac{1}{4\pi\varepsilon_0}\frac{Zq}{r^3}\right)\mathbf{v}\times\mathbf{r} = -\frac{1}{c^2}\left(\frac{1}{4\pi\varepsilon_0}\frac{Zq}{r^3}\right)\mathbf{v}\times\mathbf{r} \quad \text{Where } \varepsilon_0\mu_0 = \frac{1}{c^2} \tag{87}$$

And in Equation 87, μ_0 is the vacuum magnetic permeability which in MKS units is

$$\mu_0 = 4\pi\times10^{-7}\,\frac{\text{Newton}}{\text{Ampere}^2} = 4\pi\times10^{-7}\,\frac{\text{Newton}}{(\text{Coulomb/second})^2} \text{ (Tipler and Llewellyn, 2012)} \tag{88}$$

This results in the energy splitting ΔE, referred to as spin-orbit **S·L** coupling, in the following expression given in the vector dot product below after the substitution of Equation 87 for magnetic field **B**.

$$\Delta E = -\boldsymbol{\mu}_s\cdot\mathbf{B} = -\left(-\frac{g_s\mu_b}{\hbar}\right)\mathbf{S}\cdot\left[-\frac{1}{c^2}\left(\frac{1}{4\pi\varepsilon_0}\frac{Zq}{r^3}\right)\mathbf{v}\times\mathbf{r}\right] = -\frac{g_s\mu_b}{\hbar}\mathbf{S}\cdot\left[\frac{1}{c^2}\left(\frac{1}{4\pi\varepsilon_0}\frac{Zq}{r^3}\right)\mathbf{v}\times\mathbf{r}\right] \tag{89}$$

In the frame of reference of the atomic nucleus at rest, there is the Thomas precession (Walker et al, 2014) arising from the relativistic transformation of velocities, so the spin-orbit interaction in Equation 89 is multiplied by $1/2$.

$$\Delta E = -\frac{1}{2}\frac{g_s\mu_b}{\hbar}\mathbf{S}\cdot\left[\frac{1}{c^2}\left(\frac{1}{4\pi\varepsilon_0}\frac{Zq}{r^3}\right)\mathbf{v}\times\mathbf{r}\right] \tag{90}$$

Then multiply the right-hand side of Equation 90 with the charge ratio $\frac{q}{q}(=1)$ which will be useful for incorporating the unitless parameter α.

$$\Delta E = -\frac{1}{2}\frac{g_s\mu_b}{q\hbar c^2}\left(\frac{1}{4\pi\varepsilon_0}\frac{Zq^2}{r^3}\right)\mathbf{S}\cdot(\mathbf{v}\times\mathbf{r}) \tag{91}$$

Since the electron orbital angular momentum vector **L** being equal to $\mathbf{r}\times m_e\mathbf{v}$, such that $-\mathbf{L}=m_e\mathbf{v}\times\mathbf{r}$ because the cross product of two vectors anti-commute $(\mathbf{A}\times\mathbf{B})+(\mathbf{B}\times\mathbf{A})=\mathbf{0}$ (Wangness, 1986), Equation 91 becomes the following.

$$\Delta E = \frac{1}{2}\frac{g_s\mu_b}{q\hbar m_e c^2}\left(\frac{1}{4\pi\varepsilon_0}\frac{Zq^2}{r^3}\right)\mathbf{S}\cdot\mathbf{L} \tag{92}$$

Since experimentally g_s has been observed to be equal to 2 and the Bohr magneton μ_b of the electron is equal to $\mu_b = \frac{q\hbar}{2m_e}$ Equation 92 is the next expression.

$$\Delta E = \frac{1}{2m_e^2c^2}\left(\frac{1}{4\pi\varepsilon_0}\frac{Zq^2}{r^3}\right)\mathbf{S}\cdot\mathbf{L} \tag{93}$$

To determine what the vector dot product **S**·**L** is equal to, it is important to note that the total angular momentum **J** is equal to the sum of the **L** and **S** quantized angular momenta, **L** the orbital angular momentum vector and **S** the spin angular momentum vector of the electron.

$$\mathbf{J} = \mathbf{L} + \mathbf{S} \tag{94}$$

Performing the vector dot product **J**·**J** to obtain the following expression since vectors **L** and **S** are not orthogonal

$$\mathbf{J}\cdot\mathbf{J} = \mathbf{L}\cdot\mathbf{L} + \mathbf{S}\cdot\mathbf{S} + 2\mathbf{S}\cdot\mathbf{L} \tag{95}$$

This shows the following.

$$\mathbf{S}\cdot\mathbf{L} = \frac{\mathbf{J}\cdot\mathbf{J} - \mathbf{L}\cdot\mathbf{L} - \mathbf{S}\cdot\mathbf{S}}{2} = \frac{J^2 - L^2 - S^2}{2} \tag{96}$$

And since the magnitude of the dot products for each angular momentum vector **J**, **L**, and **S** with itself are the following expressions (Tipler and Llewellen, 2012),

$$\mathbf{J}\cdot\mathbf{J} = J^2 = j(j+1)\hbar^2 \qquad \mathbf{L}\cdot\mathbf{L} = L^2 = l(l+1)\hbar^2 \qquad \mathbf{S}\cdot\mathbf{S} = S^2 = s(s+1)\hbar^2 \tag{97}$$

Equation 93 becomes

$$\Delta E = \frac{\hbar^2}{4m_e^2c^2}\left(\frac{1}{4\pi\varepsilon_0}\frac{Zq^2}{r^3}\right)[j(j+1) - l(l+1) - s(s+1)] \tag{98}$$

Concerning Equation 98, for $j = l + \frac{1}{2}$, ΔE is

$$\Delta E = \frac{\hbar^2}{4m_e^2c^2}\left(\frac{1}{4\pi\varepsilon_0}\frac{Zq^2}{r^3}\right)\left[\left(l+\frac{1}{2}\right)\left(l+\frac{3}{2}\right) - l(l+1) - \frac{1}{2}\left(\frac{1}{2}+1\right)\right] = \frac{\hbar^2}{4m_e^2c^2}\left(\frac{1}{4\pi\varepsilon_0}\frac{Zq^2}{r^3}\right)l > 0 \tag{99}$$

And for $j = l - \frac{1}{2}$, ΔE equals the following equation representing a lower energy state for $l - \frac{1}{2}$

$$\Delta E = \frac{\hbar^2}{4m_e^2c^2}\left(\frac{1}{4\pi\varepsilon_0}\frac{Zq^2}{r^3}\right)\left[\left(l-\frac{1}{2}\right)\left(l+\frac{1}{2}\right) - l(l+1) - \frac{1}{2}\left(\frac{1}{2}+1\right)\right] = -\frac{\hbar^2}{4m_e^2c^2}\left(\frac{1}{4\pi\varepsilon_0}\frac{Zq^2}{r^3}\right)(l+1) < 0 \tag{100}$$

Now we have the expression in Equation 98 for the spin-orbit **S**·**L** coupling term that can be transformed in units of electron rest mass energy m_ec^2 as in Equations 52 for the quantum energy levels E_s of the relativisticSchrödinger differential wave equation. First, transform r into unitless ρ, since $r = \frac{\rho}{2\beta}$, by the following transformations of Equation 98 with substitution of $\alpha = \frac{q^2}{\hbar c 4\pi\varepsilon_0} = \frac{1}{137.036}$.

$$\Delta E = \frac{\hbar^3}{4m_e^2c}(2\beta)^3\frac{Z\alpha}{\rho^3}[j(j+1) - l(l+1) - s(s+1)] \tag{101}$$

$$\Delta E = \frac{2\hbar^3}{m_e^2c}\beta^3\frac{Z\alpha}{\rho^3}[j(j+1) - l(l+1) - s(s+1)] \tag{102}$$

Then substitute β^2 form Equation 48 into $\beta^3=(\beta^2)^{3/2}$

$$\Delta E = \frac{2\hbar^3}{m_e^2 c}\left(\frac{m_e^2c^4 - E_s^2}{\hbar^2c^2}\right)^{\frac{3}{2}}\frac{Z\alpha}{\rho^3}[j(j+1) - l(l+1) - s(s+1)] \tag{103}$$

One then substitutes Equation 52 for E_s and after performing some algebraic operations, Equation 103 becomes

$$\Delta E = m_e c^2 \frac{2Z\alpha}{\left(1+\frac{\gamma_{nl}^2}{Z^2\alpha^2}\right)^{\frac{3}{2}}}[j(j+1) - l(l+1) - s(s+1)]\frac{1}{\rho^3} \tag{104}$$

Then perform an integration, either numerically or use the analytical solutions for $l>0$ radial wave functions, to obtain the expectation value $\langle\frac{1}{\rho^3}\rangle$ evaluate the expectation value $\langle\Delta E\rangle$ of ΔE due to the wave characteristics of an electron in the atom.

$$\langle\frac{1}{\rho^3}\rangle = \int_0^\infty R(\rho)\frac{1}{\rho^3}R(\rho)\rho^2 d\rho \tag{105}$$

$$\langle\Delta E\rangle = m_e c^2 \frac{2Z\alpha}{\left(1+\frac{\gamma_{nl}^2}{Z^2\alpha^2}\right)^{\frac{3}{2}}}[j(j+1) - l(l+1) - s(s+1)]\langle\frac{1}{\rho^3}\rangle \tag{106}$$

$$\langle\Delta E_e\rangle = \frac{\langle\Delta E\rangle}{m_e c^2} = \frac{2Z\alpha}{\left(1+\frac{\gamma_{nl}^2}{Z^2\alpha^2}\right)^{\frac{3}{2}}}[j(j+1) - l(l+1) - s(s+1)]\langle\frac{1}{\rho^3}\rangle \tag{107}$$

Table VI displays the energy values including spin-orbit **S·L** coupling in the relativistic Schrödinger differential wave equations and that from the Dirac relativistic differential wave equation. Table VI also shows the experimentally observed Lamb shift (Lamb and Retherford, 1947) when using the relativistic Schrödinger differential wave equation with spin-orbit **S·L** coupling, such that the $2p_{1/2}$ orbital is slightly less in energy than the $2s$, and the same for the $3p_{1/2}$ and $3s$ orbitals as well as for the $4p_{1/2}$ and $4s$ orbitals. The Dirac relativistic differential wave equation yields these two orbitals in the n=2, n=3, and n=4 shells to be equal in energy.

The Dirac Relativistic Differential Wave Equation

In addition to the relativistic Schrödinger differential wave equation, Dirac developed a Hamiltonian for the relativistic effects of the electron in the hydrogen atom and hydrogen-like cations shown below.

$$\mathbf{H}\begin{bmatrix}\psi_a(r)\\ \psi_b(r)\end{bmatrix} = \begin{bmatrix} -\frac{1}{4\pi\varepsilon_0}\frac{Ze^2}{r} + m_e c^2 & -icp_r - c\frac{\hbar}{r} - \frac{c\hbar j'}{r} \\ icp_r + c\frac{\hbar}{r} - \frac{c\hbar j'}{r} & -\frac{1}{4\pi\varepsilon_0}\frac{Ze^2}{r} - m_e c^2 \end{bmatrix}\begin{bmatrix}\psi_a(r)\\ \psi_b(r)\end{bmatrix} = E\begin{bmatrix}\psi_a(r)\\ \psi_b(r)\end{bmatrix} \text{ (Dirac, 1930)} \tag{108}$$

Dirac based this upon the 2×2 matrix due to the intrinsic spin of $1/2$ in the electron. There are no spherical harmonics involving spherical polar coordinates θ and ϕ and in Equation 108, p_r and j' are the two following mathematic statements.

$$p_r = -i\hbar\frac{d}{dr} \qquad j' = j + \frac{1}{2} = \left(l \pm \frac{1}{2}\right) + \frac{1}{2} \tag{109}$$

In Equation 109, j is the sum or difference of the angular quantum number l and intrinsic spin quantum number $1/2$ for the electron in the atom. Instead of only one radial wave function, the Dirac relativistic differential wave equation has two due to the Hamiltonian being a 2×2 matrix based upon the Pauli spin matrixes of the electron intrinsic spin.

$$\psi_a(r) = \frac{1}{r}e^{-r/a}f(r) = \frac{1}{r}e^{-r/a}\sum_{k=0}^{K} f_k r^k \tag{110}$$

$$\psi_b(r) = \frac{1}{r}e^{-r/a}g(r) = \frac{1}{r}e^{-r/a}\sum_{k=0}^{K} g_k r^k \tag{111}$$

In Equations 110 and 111, a in both negative exponentials equals the following expression.

$$a = \sqrt{\left(\frac{\hbar c}{m_e c^2 - E_s}\right)\left(\frac{\hbar c}{m_e c^2 + E_s}\right)} \tag{112}$$

And the coefficients in both Equations 110 and 111 are different and have terminating series which yield the following equation for the sum energy levels E_s of the electron, which is the total mechanical energy E_m plus the rest mass energy $m_e c^2$ of the electron.

$$E_s = \frac{m_e c^2}{\sqrt{1 + \dfrac{Z^2\alpha^2}{\left[n - \left(j + \frac{1}{2}\right) + \sqrt{\left(j + \frac{1}{2}\right)^2 - Z^2\alpha^2}\right]^2}}} \tag{113}$$

It is important to note that Equation 117 will result in a complex number when the atomic number of a large nucleus has more than 137 protons for quantum number $j = \frac{1}{2}$. In comparison, Table VI displays the results by the Dirac's relativistic differential wave equation for the $1s$ to $4f$ orbitals in the hydrogen-like cation Cu^{28+} with that of the relativistic Schrödinger differential wave equations.

In addition, Table VI displays ionization energies of the hydrogen-like cation Cu^{28+} for the $1s$ to $4s$ orbitals calculated using the classical Schrödinger differential wave equation (Walker et al., 2014). However, in the classical Schrödinger differential wave equation, quantum levels with different angular momentum quantum number l are degenerate that have the same principal quantum number n when not taking spin-orbit **S·L** coupling into account. If one takes spin-orbit **S·L** coupling into account, the resulting energy values do not agree with experimental results since it is relativistic effects which cause the loss in degeneracy of the angular momentum quantum levels that have same principal quantum number n.

Conclusion

Results are reported in this paper which can match experimental ionization energies for hydrogen-like cations from numerical analyses of the relativistic Schrödinger differential wave equation if incorporating experimental ionization energies for the $1s$ electron. The likely reason why the theoretical relativistic Schrödinger differential wave equation and measurement of $1s$ ionization

energies of hydrogen-like cations differ in value is that the subatomic particles are not point masses as in the traditional treatment of wave-particle duality in quantum mechanics. For l=0 electron orbitals at any principal quantum number n, the analytical solutions for both the relativistic Schrödinger differential wave equation, assuming factor f_{ns}=1, and Dirac relativistic differential wave equation predict that the $R(\rho)$ function goes to infinity at the center of the atomic nucleus. This cannot be the real case since subatomic particles are not point masses but have very microscopic definite volumes. Both plots in Figures 2 and 3 have limited maximum values when the electron is at the center of the atomic nucleus.

This paper demonstrates the hyperfine anomalies seen in particularly large atoms which have different ionization energies. Interestingly, the experimental data generated with a numerical analysis in our work reveal the Lamb shift, which is not shown by the Dirac equation. For l=0, it is important to take into consideration that the nucleus is not a point mass and only a numerical solution with experimental data can be used to determine the shape of the orbital. While anomalies may seem irrelevant, they may explain some of the mysterious phenomena encountered in nature, such as the colors of copper and gold metals, the liquid state of mercury, and the malleability of lead. Perhaps there are other consequences of unknown anomalies in nature, which might even explain why some people see Bigfoot and others do not.

References

Arfken, George B., and Hans J. Weber. 2005. *Mathematical Methods for Physicists*. 6th Edition. Elsevier Academic Press, San Diego, CA.

Cook, Norman. 2010. *Models of the Atomic Nucleus: Unification Through a Lattice of Nucleons.* 2nd Edition. Springer-Verlag, New York.

Dirac, P.A.M. 1930. *The Principles of Quantum Mechanics*. Oxford University Press, Oxford, England.

Einstein, Albert. 1905a. Über einen die Erzeugung und Verwandlung des Lichtes betreffenden heuristischen Gesichtspunkt. Annalen der Physik 17:132-148.

Einstein, Albert. 1905b. Über die von der molekularkinetischen Theorie der Wärme geforderte Bewegung von in ruhenden Flüssigkeiten suspendierten Teilchen. Annalen der Physik 17:549-560. 21 Einstein, Albert. 1905c. Zur Elektrodynamik begetter Körper. Annalen der Physik 17:891-921.

Einstein, Albert. 1905d. Ist die Trägheit eines Körpers von seinem Energieinhalt abhängig? Annalen der Physik 18:639-641.

Eisberg, Robert, and Robert M. Resnick. 1986. *Quantum Physics of Atoms, Molecules, Solids, Nuclei and Particles*. 2nd Edition. John Wiley & Sons, Inc., Hoboken, NJ.

Kleppner, Daniel and Robert Kolenkow. 2014. *An Introduction to Mechanics*. 2nd Edition. Cambridge University Press, Cambridge, United Kingdom.

Lamb, Willis E. Robert C. Retherford. 1947. Fine Structure of the Hydrogen Atom by a Microwave Method. Physical Review. 72:241-243.

LeVeque, Randall J. 2007. *Finite-Difference Methods for Ordinary and Partial Differential Equations*. Society for Industrial and Applied Mathematics, Philadelphia, PA.

McNeill, James H., and J.E. Bidlack. 2018. Modifying the Redlich-Kwong-Soave equation of state. Proceedings of the Oklahoma Academy of Science. 98:127-138.

McNeill, James H., Robert A. Doti, and James E. Bidlack. 2021. Modern Perspectives on Einstein's General Theory of Relativity. Proceedings of the Oklahoma Academy of Science. 101:115-137.

Microsoft Corporation. 2018. Microsoft Excel. Retrieved from https://office.microsoft.com/excel. Accessed April 2025.

Miessler, Gary L., Paul A. Fischer, and Donald A. Tarr. 2014. *Inorganic Chemistry*. 5th Edition. Pearson, New York.

Tipler, Paul A. and Ralph A. Llewellyn. 2012. *Modern Physics*. 6th Edition. W. H. Freeman & Company, New York.

Walker, Jearl, Robert Halliday, and Robert Resnick. 2014. *Fundamentals of Physics*. 10th Edition. John Wiley & Sons, Inc., Hoboken, NJ.

Wangsness, Ronald K. 1986. *Electromagnetic Fields*. 1986. 2nd Edition. John Wiley & Sons, Inc., Hoboken, NJ.

Wikipedia: The Free Encyclopedia. 2025. Molar Ionization Energies of the Elements. https://en.wikipedia.org/wiki/Molar_ionization_energies_of_the_elements. Wikipedia Foundation. Accessed April 2025.

Wong, Samuel S. M. 1998. *Introductory Nuclear Physics*. 2nd Edition. John Wily & Sons, Inc., Hoboken, NJ. 22